

Infrared surface plasmon resonance biosensor

Justin W. Cleary,¹ Gautam Medhi,¹ Monas Shahzad,¹ Robert E. Peale,^{1*} Walter R. Buchwald,² Sandy Wentzell,² Glenn D. Boreman,³ Oliver Edwards,⁴ and Isaiah Oladeji⁵

¹Department of Physics, University of Central Florida, Orlando, Florida 32816, USA

²Air Force Research Laboratory, Sensors Directorate, Hanscom Air Force Base, Massachusetts 01731, USA

³College of Optics (CREOL), University of Central Florida, Orlando, Florida 32816, USA

⁴Zyberwear Inc., 2114 New Victor Rd., Ocoee, Florida 34761, USA

⁵Sisom Thin Films, LLC, 1209 West Gore Street, Orlando, FL 32805, USA

*peale@mail.ucf.edu

Abstract: A Surface Plasmon Resonance (SPR) biosensor that operates deep into the infrared (3-11 μm wavelengths) is potentially capable of biomolecule recognition based on both selective binding and characteristic vibrational modes. The goal is to operate such sensors at wavelengths where biological analytes are strongly differentiated by their IR absorption spectra and where the refractive index is increased by dispersion. This will provide enhanced selectivity and sensitivity, when biological analytes bind reversibly to biomolecular recognition elements attached to the sensor surface. This paper investigates potentially useful IR surface plasmon resonances on lamellar gratings formed from various materials with plasma frequencies in the IR wavelength range including doped semiconductors, semimetals, and conducting polymers. Water is found to broaden the IR plasmon resonance significantly at 9.25 μm where aqueous extinction is large. Much sharper resonances for IR biosensing can be achieved in the 3.5 to 5.5 μm range.

© 2010 Optical Society of America

OCIS codes: (240.6680) Surface plasmons; (280.1415) Biological sensing and sensors; (130.3060) Infrared; (130.5990) Semiconductors; (050.2770) Gratings.

References and links

1. J. W. Cleary, G. Medhi, R. E. Peale, W. R. Buchwald, O. Edwards, and I. Oladeji, "Infrared surface plasmon resonance biosensor," *Proc. SPIE* 767306 (2010).
2. J. W. Cleary, R. E. Peale, D. J. Shelton, G. D. Boreman, C. W. Smith, M. Ishigami, R. Soref, A. Drehman, and W. R. Buchwald, "IR permittivities for silicides and doped silicon," *J. Opt. Soc. Am. B* **27**, 730-734 (2010).
3. R. Soref, R. E. Peale and W. Buchwald, "Longwave plasmonics on doped silicon and silicides," *Opt. Express* **16**, 6507-6514 (2008).
4. J. W. Cleary, G. Medhi, R. E. Peale, G. D. Boreman, S. Wentzell, and W. R. Buchwald, "Infrared surface plasmons on antimony," *J. Opt. Soc. Am. B* (submitted 2010).
5. J. W. Cleary, G. Medhi, R. E. Peale, and W. R. Buchwald, "Long-wave infrared surface plasmon grating coupler," *Appl. Opt.* **49**, 3102-3110 (2010).
6. J. Cleary, R. E. Peale, D. Shelton, G. Boreman, R. Soref, W. Buchwald, "Silicides for infrared surface plasmon resonance biosensors," *Proc. Mat. Res. Soc.* 1133-AA10-03 (2008).
7. K. Lee, S. Cho, S. H. Park, A. J. Heeger, C. Lee, and S. Lee, "Metallic transport in polyaniline," *Nature* **441**, 65-68 (2006).
8. M. A. Ordal, R. J. Bell, R. W. Alexander Jr., L. L. Long and M. R. Querry, "Optical properties of Au, Ni, and Pb at submillimeter wavelengths," *Appl. Opt.* **26**, 744-752 (1987).
9. D. W. Lynch and W. R. Hunter, "Gold (Au)," in *Handbook of optical constants of solids*, E. D. Palik, ed. (Academic Press, Orlando, FL, 1985).
10. S. M. Sze, *Physics of semiconductor devices 2nd ed.* (Wiley-Interscience, New York, NY, 1981).
11. W. L. Wolfe, "Optical materials," in *Handbook of military infrared technology*, W. L. Wolfe, ed. (Office of Naval Research, Washington D.C., 1965).

12. Y. Marechal, "Infrared spectra of water. I. Effect of temperature and of H/D isotopic dilution," J. Chem. Phys. **95**, 5565-5573 (1991).

1. Introduction

A Surface Plasmon Resonance (SPR) biosensor for identifying and quantifying bio-molecules and their interactions that operates deep into the infrared (3-11 μm wavelengths), has potential for recognition based both on selective binding and characteristic vibrational modes. The idea is to operate specifically at wavelengths where biological analytes are strongly differentiated by their IR absorption spectra. In comparison with current commercial visible/near-IR systems, enhanced sensitivity and selectivity are anticipated due to large index changes known to accompany IR absorption features. The proposed IR SPR biosensor will have applications in life science, electro-analysis, drug discovery, food quality and safety, environmental science, gas-and liquid-phase chemical sensors, forensics, defense, and security.

Biomolecules that adhere to a conducting surface strongly affect the bound electromagnetic waves known as surface plasmon-polaritons (SPP), providing a means for real-time label-free sensing and monitoring of biological entities from molecules to cells. Current commercial systems are based on angle-dependent resonant absorption at the surface of gold-coated attenuated total reflection (ATR) prisms under conditions of total internal reflection. Our experiments [1] show that grating couplers are advantageous in the IR since they are easy to fabricate photolithographically, and the thickness of the conducting layer is arbitrary as long as it is optically thick. Additionally, incident light passes through less lossy media before reaching the surface when compared to the more typical ATR configuration.

Fig. 1 presents a schematic of a grating based SPR biosensor. A monochromatic, p-polarized IR light source is focused through a flow channel and onto a conducting diffraction grating. The intensity of the reflected light is analyzed by an array detector as a function of incident angle. The top surface of the conducting grating is functionalized with biomolecule recognition elements that reversibly capture specific analyte biomolecules from the flow channel. This results in a refractive index change within a few 100 nm of the surface, which is sensed by the SPP field, causing a shift in the SPP resonance angle.

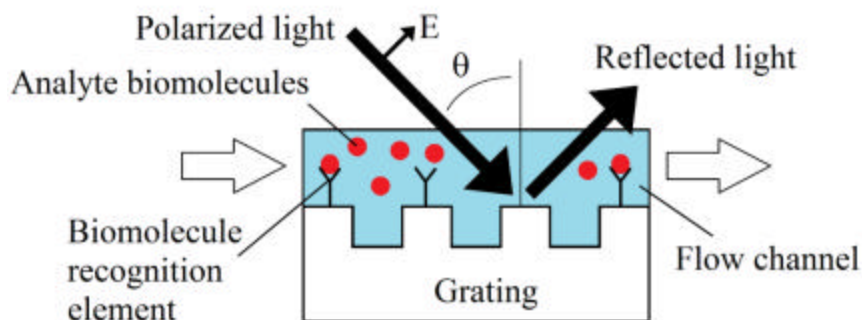


Fig. 1. Schematic of grating based SPR Biosensor.

For IR operation, (3 to 11 μm), one might use (for example) a quantum cascade laser as a narrow band light source, a doped silicon grating as the conducting surface, all-silicon microfluidic channels and controls, and an IR, 2-D array detector. In comparison to gold, the lower plasma frequency of doped silicon allows IR SPP fields to be $\sim 10\times$ more confined to the sensor surface, (i.e. to within ~ 10 nm), so that there is good spatial overlap between the plasmon fields and the biological analyte-ligand.

Previously, SPP field confinement on doped silicon [2,3] and antimony [4] has been investigated. This paper describes optical investigation of new IR SPP hosts. Materials with

plasma frequencies one order of magnitude smaller than for noble metals are considered, including doped semiconductors, semimetals, and conducting polymers.

2. Background

Gratings are well known as couplers between photons and SPPs [5]. They function by shifting the incident photon wavevector by integer multiples, m , of $2\pi/a$, where a is the grating period. This wavevector shift compensates for the inherent momentum mismatch that exists between free space optical fields and SPP's. Grating couplers have the additional feature of allowing multiple resonant SPP excitations to occur due to the multiple units of grating momentum that may be added to the incident wavevector.

Previously, a number of different conductors were considered for use as IR SPP hosts due to their superior mode confinement when compared to traditional noble metals. We have published theoretical and experimental studies of doped-Si [1-3], metal silicides [2,3,6] and the semi-metal antimony [1,4]. In this work we also consider the semiconductor CuSnS, the semimetals graphite and Bi, and the conducting polymer polyaniline. We also present new results for doped-Si and include the noble metal Au for comparison purposes.

Gratings of 20 μm period, 50% duty and different heights were formed by photolithography and plasma etching. For Au, Bi and Sb, an optically thick layer of material was thermally evaporated onto patterned Si substrates. The graphite grating was plasma etched directly into a crystalline graphite substrate. CuSnS gratings were formed by wet-chemical deposition on patterned Mo substrates. Actual grating heights were determined by a profilometer.

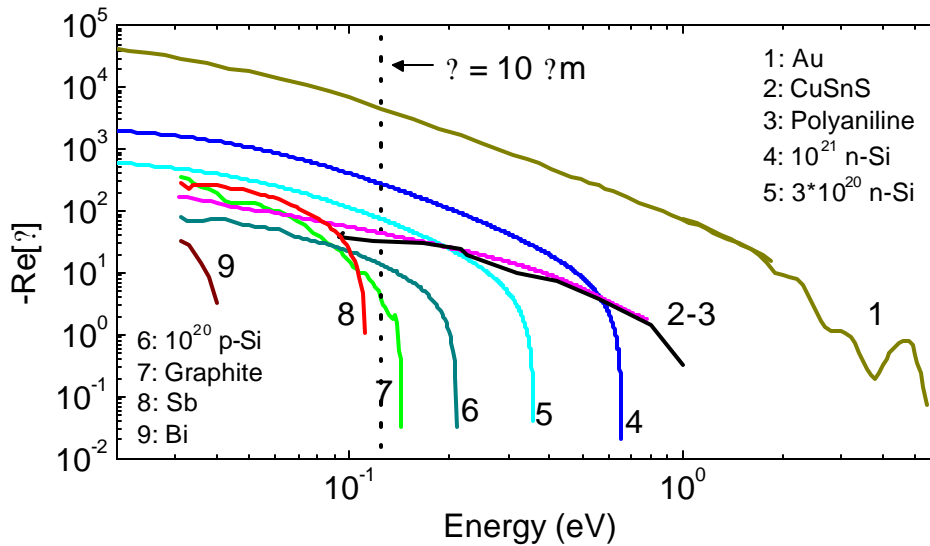


Fig 2. Real part of the permittivity as measured by ellipsometry for CuSnS, graphite, Bi, Sb, p-Si. Published permittivity for doped polyaniline is included [7]. Values for Au are included for comparison purposes [8, 9]. The curves for n-Si are calculated from the Drude model. The doped-Si carrier concentrations are noted in the legend. The energy corresponding to 10 μm free space wavelength is indicated.

Angular reflectance spectra were measured using a goniometer, a quantum cascade laser (9.38 μm) or CO₂ laser (9.250 μm), along with a power meter or a HgCdTe detector operating at 77K. In all cases gratings of $\sim 1 \mu\text{m}$ height gave the strongest resonances, but the resonances for smaller heights are sharper. More details of the reflectance measurement method used here are given in [5].

Fig. 2 presents the real part of the permittivity, ϵ' , from ellipsometry measurements on CuSnS, doped polyaniline [7], Graphite, Sb [4], Bi and p-Si. Theoretical curves for n-Si are also presented. Published Au permittivity values are included for comparison [8,9]. The wavelength of $10 \mu\text{m}$ is indicated by a vertical line. Most conductors with IR plasma frequencies have an imaginary part, ϵ'' , which is comparable to or higher than the real part suggesting that resonances may be broad. Expected resonance angles and the angular reflectance spectra are calculated using the ϵ' and ϵ'' values according to analytic formulas described in [5].

3. Experiment and results

Fig. 3 (top-left) presents optimized calculated resonance spectra for n-Si with different carrier concentrations at the CO_2 laser wavelength of $9.250 \mu\text{m}$. Evidently, to see a clear resonance, a concentration of at least 10^{20}cm^{-3} is required. Fig. 3 (bottom-left) presents a measured resonance spectrum for a $1 \mu\text{m}$ high grating etched in p-Si wafers with resistivity $0.0006 - 0.001 \Omega\text{-cm}$. Such material has a carrier concentration in the range of $1-2 \times 10^{20} \text{cm}^{-3}$ [10]. The measurement is in reasonable agreement with the calculation.

Fig. 3 (top-right) shows the optimized calculated resonance for a CuSnS grating at our QCL wavelength of $9.38 \mu\text{m}$. The measured angular reflectance spectrum of a $3 \mu\text{m}$ high CuSnS grating is presented in Fig. 3 (bottom-right). A resonance appears in the expected angular position, as indicated by the symbol. The grating height of $3 \mu\text{m}$ is too large for optimum SPP coupling [5], so that the measured resonance line shape agrees poorly with the optimized calculation.

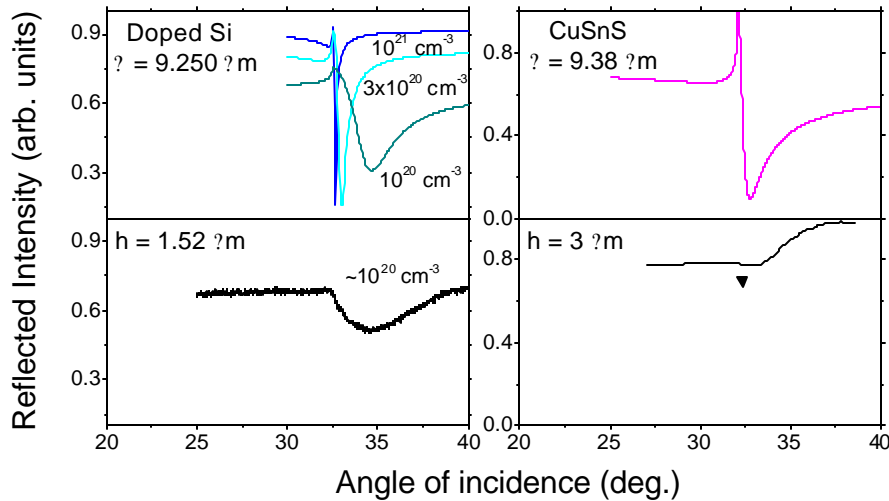


Fig. 3. (top-left) Calculated reflectance spectra for n-type Si gratings with varying carrier concentrations. (bottom-left) Measured angular reflectance spectra for a p-type Si lamellar grating with $1 \mu\text{m}$ height. (top-right) Calculated reflectance spectra for a CuSnS grating. (bottom-right) Measured angular reflectance spectra for a CuSnS lamellar grating of with $3 \mu\text{m}$ height. A symbol indicates the calculated resonance angle.

The optimized calculated reflectance spectrum for a graphite grating [5] shows a reasonably sharp and deep resonance (Fig. 4 left-top). The calculated penetration depth for the SPP field into air above the graphite surface is $23 \mu\text{m}$ at $10 \mu\text{m}$ wavelength. This is larger than for heavily-doped silicon but smaller than for silicides or noble metals. The measured angular reflectance spectrum for a $0.2 \mu\text{m}$ high graphite grating is presented in Fig. 4 (left-center). The resonances are very weak but appear near the calculated resonance angles

(symbols). The grating height of $0.2 \mu\text{m}$ is too small for optimum SPP coupling [5], so that the measured resonances line shape agrees poorly with the optimized calculation.

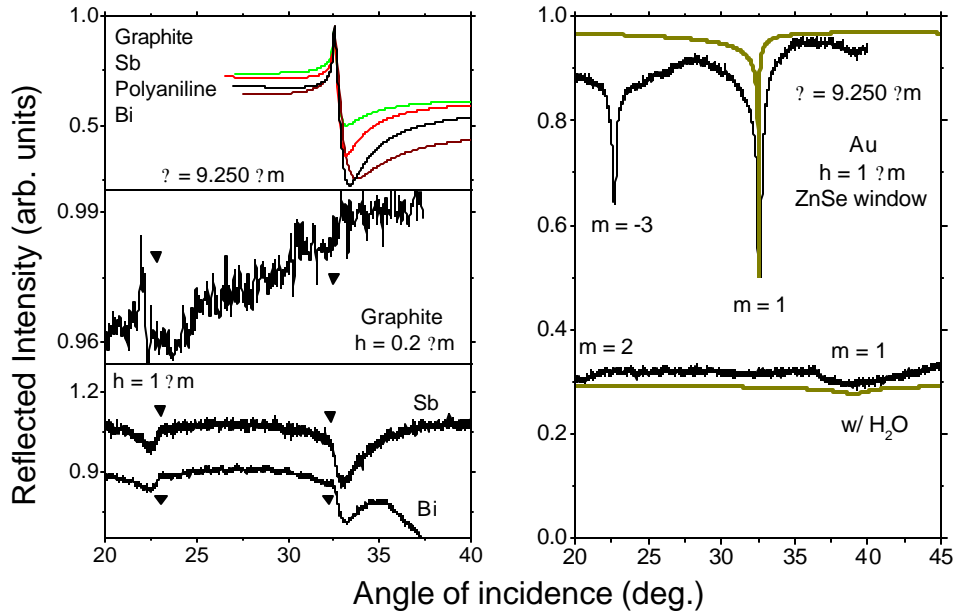


Fig. 4. (left-top) Optimized calculated reflectance spectra for Graphite, Sb, polyaniline and Bi gratings. The indicated ordering of the curves is the same on both sides of the resonance. (left-center) Measured angular reflectance spectra for a Graphite lamellar grating of with $0.2 \mu\text{m}$ height. (left-bottom) Measured angular reflectance spectra for Sb and Bi lamellar gratings of with $1 \mu\text{m}$ height. Symbols represent the calculated resonance angles. (right) Measured angular reflectance spectra for a Au lamellar grating with $1 \mu\text{m}$ height with an attached ZnSe window, with and without H_2O filling the gap between grating and window. Curves without noise are calculations.

Bi gratings show clear SPP resonances in calculations (Fig. 4 left-top) and in measurements (Fig. 4 left-bottom). The Bi grating amplitude was $1 \mu\text{m}$. The same figure shows that a similar situation holds for Sb. A $1 \mu\text{m}$ grating amplitude is close to optimum, so that the measured resonance profile agrees well with the optimized calculation [4].

An optimized reflectance calculation for polyaniline (Fig. 4 left-top) gives a resonance that is deeper and sharper than those for Sb, Bi and Graphite gratings.

Water, the usual media in biosensor applications, has considerable dispersion in the IR, and values for n are significant. Hence, we expect the resonances to be both shifted and broadened for wet gratings in comparison to dry ones. To investigate this experimentally, a $1 \mu\text{m}$ amplitude Au grating was prepared. A ZnSe window was attached in contact with the grating. A drop of water placed at the edge of the window flowed by capillary attraction into the gap, providing a uniform layer. The reflected laser intensity was observed to decrease by a factor of ~ 3 due to absorption by water, which was used to estimate that the water layer thickness was $\sim 10 \mu\text{m}$. Fig. 4 (right) presents measured reflectance spectra, both wet and dry. The resonances are labeled by the number of the grating quanta involved. Both initial dry resonances are sharp, but water broadens and shifts them significantly. The experimental observations agree with calculations.

Fig. 5 (left) presents the extinction coefficient of water [11]. The wavelength $9.25 \mu\text{m}$ is indicated in Fig. 5 (left) by an arrow. An extinction coefficient nearly an order of magnitude smaller is found at $3.9 \mu\text{m}$. Fig. 5 (right) presents a calculated resonance spectrum for the wet

conditions in Fig. 4 (right) but at 3.9 μm wavelength. This resonance is sharp. We identify the range 3.5 – 5.5 μm as that best suited for an IR SPR biosensor with H_2O . If D_2O is used, the best suited range shifts to 4.5 – 8 μm [12]. Hence, the choice of using H_2O or D_2O as an analyte carrier depends on the IR region where vibrational modes of biomolecules are expected.

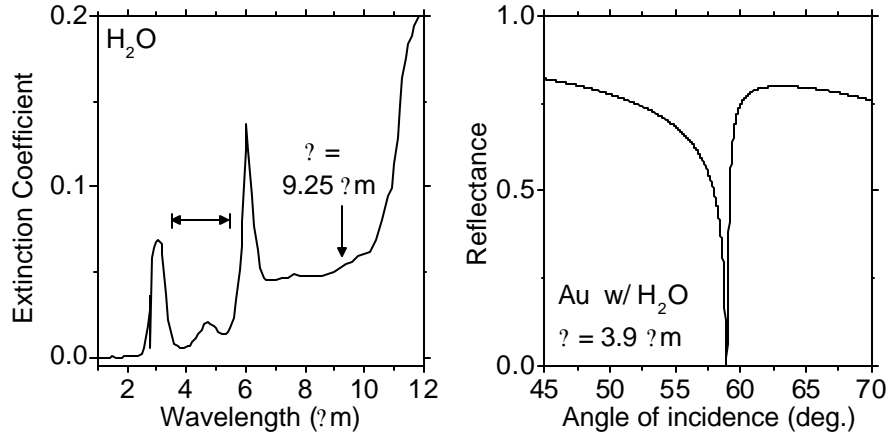


Fig. 5 (left) Extinction coefficient of water in the IR from [11]. The wavelength used to measure the gold grating in water is indicated by an arrow. The wavelength range with the smallest extinction coefficient for water in the mid-IR is indicated. (right) Calculated resonance spectrum for a Au grating with water at 3.9 μm .

4. Conclusion

Calculated and experimental SPP resonances on semiconductor, semi-metal and conducting polymer gratings in the IR were presented. All show reasonable prospects as SPP hosts in the IR with sufficient mode confinement for sensor applications. Wetting the grating shifts and broadens the SPP resonances significantly at 9.25 μm . To maintain sharp SPR resonances, the ideal range for an IR SPR biosensor would be 3.5 – 5.5 μm .

Acknowledgments

This project is supported by an NSF Phase I SBIR and by an AFOSR grant FA95501010030 (Gernot Pomrenke PM).